Optimized Porous Anodic Alumina Membranes for Water Ultrafiltration of Pathogenic Bacteria (E. coli)

Article *in* Journal of Nanoscience and Nanotechnology · June 2016

DOI: 10.1166/jnn.2016.11034

10 authors, including:

Maria manuela Machado
Universidade Presbiteriana Mackenzie
5 PUBLICATIONS **14** CITATIONS
SEE PROFILE

Mônica Rosas da Costa Iemma
Universidade Federal de São Carlos
15 PUBLICATIONS **171** CITATIONS
SEE PROFILE

Dulce H F Souza
Universidade Federal de São Carlos
38 PUBLICATIONS **577** CITATIONS
SEE PROFILE

Caue Ribeiro
Brazilian Agricultural Research Corporation (EMBRAPA)
207 PUBLICATIONS **3,561** CITATIONS
SEE PROFILE

Article

Journal of
Nanoscience and Nanotechnology
Vol. 15, 1–9, 2015
www.aspbs.com/jnn

Optimized Porous Anodic Alumina Membranes for Water Ultrafiltration of Pathogenic Bacteria (*E. coli*)

Alexsandro Mendes Zimer[1], Maria Manuela P. Machado[1], Lázaro José Dalla Costa Júnior[1], Priscila Tomie Leme Ike[2], Mônica R. C. Iemma[2], Cíntia Fumi Yamamoto[3], Cauê Favero Ferreira[3], Dulce H. F. Souza[2], Cauê Ribeiro de Oliveira[3], and Ernesto Chaves Pereira[1,*]

[1] *Laboratório Interdisciplinar de Eletroquímica e Cerâmica (LIEC)–Federal University of São Carlos (UFSCar)–Department of Chemistry–C.P.: 676, CEP: 13.565-905, São Carlos, SP, Brazil*
[2] *Laboratório de Bioquímica Funcional e Estrutural (LBFE), -Federal University of São Carlos (UFSCar)—Department of Chemistry—C.P.: 676, CEP: 13.565-905, São Carlos, SP, Brazil*
[3] *Empresa Brasileira de Pesquisa Agropecuária (EMBRAPA), CEP. 13560-970, São Carlos, SP, Brazil*

In this paper, we present the optimization of porous anodic alumina membranes for ultrafiltration prepared by anodically oxidized aluminum foils. The membranes were characterized by field-emission scanning electron microscopy to measure the pore diameter and the membrane thicknesses. The liquid fluxes were estimated through gas permeability measurements using Darcy's and Forchheimerś equations. A 2^3 factorial design we used to optimize the membrane properties: pore diameter, membrane thickness, and liquid flux using as control variables the applied current density, solution composition and concentration. It was observed that the most import variables to control the pore diameter were current density and electrolyte composition. After the anodization both, metallic aluminum substrate and the barrier layer of alumina were removed using adequate solutions to obtain the free standing membrane. Then, *Escherichia coli* a common bacterial contamination of drinking water was removed using these PAA membranes with 100% of efficiency to obtain bacteria-free water.

Keywords: Porous Anodic Alumina Membranes, Low Cost Aluminum, Ultrafiltration, Drinking Water.

1. INTRODUCTION

The availability of drinking water has been described as one of the most important problems of the beginning of the 21st century.[1] The presence of different chemical and biological contaminants in water used for human and animal consumption leads to problems related to public health, especially for destitute populations. Water treatment systems involve coupled processes, with each part intended for the removal of one or more substances from the source water, such as the particulate material treatment process, based on the size and properties of the target contaminant.[2] However, the efficient removal of particles with sizes less than 1 μm can not be done in large scale systems and, as consequence, the drinking water purification installations cannot effectively retain pathogens,[3] which have sizes less than 0.2 μm.

Currently, nanoporous membranes have been used because of their effectiveness in removing contaminants without the production of byproducts, particularly in water treatment processes of water and wastewater. The basic principle of membrane filtration is to use semi-permeable membranes to remove fluids, gases, particles, and solutes. For the separation of these substances from water, the membrane must be water-permeable and non-permeable to the solutes or particles. In this sense, different membrane processes can actually be founded for water treatment, reuse, and desalination, including microfiltration,[4] ultrafiltration (UF),[5] and nanofiltration process.[6,7] In the case of membranes to be used in UF, different materials have been proposed, such as, ceramic materials,[5] polymers,[8] and oxides.[9–11]

The removal of viruses and bacteria from drinking water is extremely important to ensure the quality of water for human and animal consumption.[12] While chlorination is

*Author to whom correspondence should be addressed.

still the most common method of disinfection, it causes the formation of byproducts, such as chlorine and chloramines (DBPs), and, besides, *Cryptosporidium oocysts* is resistant to it.[3] The removal of *Escherichia coli* from drinking water using carbon nanotube (CNT) membranes was efficiently conducted by Srivastava et al.[13] In their studies CNTs acts as the pores in the membrane. However, it is necessary to modify CNT to allow their reuse, to increase its resistance and durability against pH changes and high concentrations of chemical compounds.[2] Besides, it is necessary a cost optimization of membranes to ultra and nanofiltration of drinking water in large scale.

Porous anodic alumina (PAA) is a material that has viable characteristics for use in sterilization systems for water treatment because of its self-ordered structure with pores of constant size in the nanometer range.[14, 15] This material has been studied for many decades[16–18] due to their unique chemical, thermal, mechanical stability,[9] optical characteristics,[19] and especially for the possibility to control the pore diameter.[20] Due their characteristics, PAA have attracted considerable interest for applications in many fields, including as templates for synthesis and/or catalysis,[21–23] molecular separation,[20] adsorption,[24] biosensing,[25–27] energy storage,[28–30] drug distribution,[31] gas separation,[10, 11, 32, 33] optical sensors,[19] and as inorganic membranes for water UF.[8, 34]

PAA membranes are synthesized by anodization of aluminum (Al) substrates in acidic aqueous solution, such as oxalic, sulphuric, chromic, or phosphoric acids,[7] resulting in membranes with a uniform, strait, cylindrical pore structure. The mechanism of pore formation has been investigated in detail by many authors.[16, 18, 35, 36] Generally, the resulting membranes have a uniform, cylindrical pore structure that results from the self-ordered growth, i.e. closely packed hexagonal cells that can be obtained under specific anodization conditions,[36] especially when "ultrapure" Al foil is used. Nevertheless, the "cost of production" has not been a focus of studies in the literature for optimization of membranes for UF of drinking water using a low-cost Al.

Low cost aluminum is scarcely investigated in the literature. Lee and Mattia[7] show the potenciostatic anodization of tubular aluminum (99.5% purity), in sulfuric and oxalic acids, and its study for UF application, i.e., bovine serum albumin rejection. Asymmetric tubular alumina membranes were successful obtained and permeability analysis shows great potential for biomolecule separation that overcomes commercial ceramic membranes.

A modified PAA membrane with a uniform carbon deposition on the inner-surface of the channels obtained through the pyrolytic decomposition of propylene was performed by Kiotany et al.[37] Chemical modification of carbon film was performed through fluorination or HNO_3 treatment. Separation of water/ethanol mixture showed that water preferentially permeated only on the fluorinated film.

Kobayashi et al.[10] reported the anodization of an Al tube (99.5% purity) in 4 wt% aqueous $H_2C_2O_4$ electrolyte. PAA membranes were characterized by scanning electron microscopy (SEM) and gas permeability measurements. According to the author the final tubular membrane, with a pore diameter of 150 nm, is more indicated for UF process, but experiments intended to set a tunable size for this nanostructure were not shown.

Considering what was described above, in this work, we present the development and optimization of low cost PAA membranes by galvanostatic anodization of commercial Al foils (99.5% purity), and their application as membrane filters in the UF process of drinking water. A 2^3 factorial design was employed to determine the best condition for the anodization step allowing for the production of adequate pore size for this purpose. The membrane morphology was characterized by field-emission scanning electron microscope (FE-SEM), and gas permeability measurements to estimate the liquid flux through the membrane. Furthermore, the PAA membranes were used UF process of bacterial contaminants, such as *E. coli*, from drinking water.

2. EXPERIMENTAL PROCEDURE

2.1. Membrane Preparation and Characterization

The aluminum foil substrate that we used was chosen based on the following three criteria: (i) cost, (ii) thickness, and (iii) mirroring of the surface. The first characteristic is necessary to guarantee the whole filtration systems remains accessible for different uses. Therefore, instead of using ultrapure aluminum foil, we decided to use 1050 Al foils (99.5% purity) that had a thickness of 25 μm (brand ALUMIESTE) available in markets as foils. The second characteristic is related to the production of membranes with adequate mechanical resistance. Finally, the last characteristic is to avoid an additional step in the preparation of membranes, such as electropolishment, once the Al sample chosen must have a flatted surfaced to satisfy the last criterion.[20]

The PAA were prepared by two-step anodization experiments (steps A to D in Fig. 1), as described by Masuda and Fukuda,[9] by exposing a circular area (diameter = 2.3 cm) of Al foil. A Teflon® cell (Volume of 200 mL) with two independent temperature control devices was used. The first control system was positioned in the solution, whereas the second one is positioned under the Al substrate to keep the temperature constant. The solution temperature was kept at 20 °C with mechanical stirring and the Al foil was kept at 10 °C using a Peltier® plaque (model DV-40-10) by setting the voltage and current to 5 V and 3 A. In the literature,[15] a similar procedure has been used to set an appropriate temperature at the Al electrode to allow for indirect control of the current density during accelerated mild anodization experiments. According to Kashi et al.,[15] it is important to remove the heat generation in

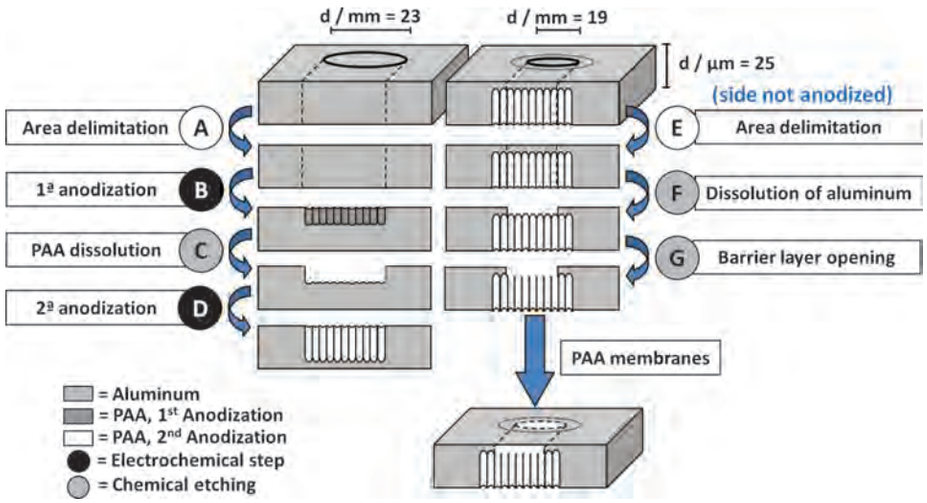

Figure 1. Flowchart describing all of the steps for the production of the final PAA membrane.

the electrode metal itself and then suppress warming of the barrier layer, which leads to a decrease in the number of the branched pores. Lee et al.[38] also proposed that heat removal avoids current and voltage changes and, therefore, leads to constant pore diameters and pore distances.

In the present work, pore diameter (D_P) optimization was performed using a 2^3 factorial design with three variables (factors) and two values.[39] The factors and their values are presented in Table I.

The first anodization step was carried out for 0.5 or 1 h under gavanostatic conditions in oxalic or phosphoric acids, respectively, using a home-made DC power supply (step A and B in Fig. 1). The porous alumina layer was then stripped away from the Al substrate by chemical etching using 0.2 mol dm^{-3} CrO_3 (Merck) in aqueous 0.4 mol dm^{-3} H_3PO_4 (Mallinckrodt) at 60 °C for 1 h under stirring. As proposed in the literature,[9] this step removes the non-ordered pores and lets a dimple array to the next anodization stage (step C in Fig. 1). The second anodization step (step D in Fig. 1) was carried out under the same conditions for 1.5 or 2.5 h in oxalic or phosphoric acids, respectively (see also Table I). These two time anodization were used because the pore growth rate is slower in phosphoric than in oxalic acid.[40] After the second anodization step, the aluminum back side of the electrode was submitted to chemical dissolution in a 0.1 mol dm^{-3} solution of $CuCl_2$ (Merck) in 20% HCl (Quemis; % by volume), to reveal the PAA barrier oxide layer (steps E and F in Fig. 1). To provide stable mechanical support to the PAA membrane, step E in Figure 1 was performed in a reduced area (diameter of 1.9 cm) compared with the anodized side of the Al foil.[35] Finally, to remove the barrier layer, a 5% H_3PO_4 (Mallinckrodt) solution (% by volume) was used as showed in step G of Figure 1. This solution, at room temperature, was applied for 15 min over the barrier layer, which was then rinsed with deionized water, and then dried under ambient conditions.

The barrier layer opening was studied in a 0.3 mol dm^{-3} solution of H_3PO_4 to determine the best condition for step G. We concluded from FE-SEM analysis (ZEISS, mod. DSM 940) that would be necessary to repeat this procedure four times to obtain an open membrane. Is important to highlight that the other side of the foil (i.e. the porous membranes) was keep safe by application of a few drops of an acetate buffer solution[35] (pH 7.0) to neutralize the acid solution from the barrier layer opening procedure. Even using such approach, the barrier layer opening was studied by FE-SEM analysis in all experimental conditions of Table I to verify the general opening efficiency of the barrier layer. Using ImageJ software the percentage of pore opening in each measurement was estimated.

Table I. Variables (factors) and levels of the 2^3 factorial design with matrix combining all of the variables and effects and the evaluated responses from the system.

		Values	
Variables	Factors	−1	1
1	Current density (mA cm^{-2})	3	8
2	[Acid] (mol dm^{-3})	0.1	0.5
3	Electrolyte	Phosphoric Acid[a]	Oxalic Acid[b]

2^3 Factorial design

Exp.	*Factor 1* j (mA cm^{-2})	*Factor 2* M_{acid} (mol dm^{-3})	*Factor 3* Electrolyte	Responses
1	−1	−1	−1	Pore
2	1	−1	1	diameter
3	−1	−1	1	(nm)
4	1	−1	−1	Thickness
5	−1	1	1	(μm)
6	1	1	−1	
7	−1	1	−1	Flux
8	1	1	1	(L h^{-1})

Notes: [a]Mallinckrodt; [b]Sigma-Aldrich.

To determine the morphological parameters of PAA membranes, such as D_p and membrane thickness (H), FEG-SEM micrographs were used with the top and cross section data, respectively. The effective D_p was determined by analyzing the total pore area from the FEG-SEM images using ImageJ software to estimate the average pore area and from this, the average D_p. In some cases, the membrane had a double network of pores. In these cases, we selected the smaller pore network because it is limiting the flow through the membrane.[11] Double network of pores for two-step anodization under galvanostatic control was described by Oliveira et al.[41] and will not be explored here. The authors proposed that this phenomenon appeared because under galvanostatic control the dimple array left by the first anodization could change the area on the Al substrate to second step anodization. As current density is set at start of experiment, this change in the actual area becomes important and a pore mismatch could appear.[41]

To estimate the output for a liquid, flux gas permeability measurements with N_2 were performed using a flux meter (Model PR100) and Darcy's law and Forchheimeŕs equations[42] from compressible to incompressible flow, as shown by Eqs. (1) and (2), respectively.

$$\frac{P_i^2 - P_o^2}{2PH} = \frac{\mu v_s}{k_1} + \frac{\rho v_s^2}{k_2} \quad (1)$$

$$\frac{\Delta P}{H} = \frac{\mu v_s}{k_1} + \frac{\rho v_s^2}{k_2} \quad (2)$$

where, P_i (Pa) is the inlet pressure and P_o (Pa) is the output pressure of the fluid through the porous material, H (m) is the thickness of membrane, μ (Pa s) is the fluid viscosity, v_s (ms^{-1}) is the fluid velocity, k_1 (m^2) is the permeability of the porous body, ρ (kg m^{-3}) is the density of fluid, and k_2 (m) is the inertial permeability for Eq. (1), and ΔP (Pa) is the pressure gradient for Eq. (2).

Three responses were studied in the 2^3 factorial design:[39,43] D_p, H, and liquid flux (ϕ). In this procedure, k^n experiments must be accomplished, where n is the number of variables and k is the number of values of each variable. In the present case, the three variables are:

(1) current density,
(2) acid concentration, and
(3) electrolyte type.

Their two values are presented as the signals (−) and (+) in Table I to set changes in each variable. Eight experiments were performed ($2^3 = 8$ exp.) and their main and cross effects (between two and three factors) were estimated in order to set the best condition to produce membranes for ultrafiltration. The calculated effects using a factorial design are determined by a matrix calculation merging all variables at their different values.[39] A linear combination between the signals of Table I was performed to obtain the average and the main effects as well as the interaction between two and three factors. The experiments were performed in duplicate and a Student's t-distribution with 8 degrees of freedom ($\upsilon = 8$) and 95% (0.025) confidence interval, i.e. 2.306, was used to calculate the limit of confident and the standard error (SE) associated with individual responses. The results are presented in Table II described in the Results Section.

Table II. Main effects and interactions estimated for the 2^3 factorial design results.

	Estimation of variable effects	
Effects and interactions	D_p/(nm)	H/(μm)
Average ± SD	**122.7 ± 0.6**	**8.0 ± 0.5**
Main effects ± SD		
(1) Current density	**45.5 ± 11**	**4.6 ± 1.0**
(2) [Acid]	−4.0 ± 11	**−2.4 ± 1.0**
(3) Electrolyte	**−68.5 ± 11**	**2.8 ± 1.0**
Interaction of two-factors ± SD		
(1) × (2)	−1.9 ± 11	−1.7 ± 1.0
(1) × (3)	3.8 ± 11	−1.1 ± 1.0
(2) × (3)	21.6 ± 11	0.8 ± 1.0
Interaction of three-factors ± SD		
(1) × (2) × (3)	0.5 ± 11	−0.4 ± 1.0
Limit of significance (95%)	**25.4**	**2.24**

2.2. Removal of Bacteria Using PAA Membrane

Removal of bacterial contamination from water was the final test to evaluate the quality of the PAA membranes. In this step, a borosilicate glass funnel of 47 mm with a fritted glass filter support (Merck-Millipore®, model XX15 047 00) was used as vacuum filter system. The fecal bacterium *E. coli* was used in this step because it is a common pollutant of drinking water.[13] The *E. coli* strain used in this work was the *E. coli* BL21 strain transformed with the pET28a plasmid, which contains a gene that confers resistance to the antibiotic kanamycin.[44] The bacteria were preserved in cryogenic tubes in Luria-Bertani (LB) medium,[44] with 10% (v/v) glycerol, and stored at −80 °C. From this stock solution, 50 μL of the bacteria were inoculated into 50 mL LB medium supplemented with kanamycin (50 μg ml^{-1}), and this solution was maintained overnight at 37 °C with agitation. Next, 100 μL of this culture medium was added to 100 mL of sterile saline solution, NaCl 0.9% (m/v), which was named the concentrated standard of bacteria and expressed as colony forming unit (CFU; 10^0 CFU dm^{-3}). This concentrated bacteria standard was filtered by the PAA membrane, which was previously sanitized in 70% alcohol, using a vacuum pump (Marconi, model MA 057/1). The bacteria standard was used to prepare four diluted solutions (in saline solution): 10^{-1}, 10^{-2}, 10^{-3}, and 10^{-4} CFU dm^{-3}. The filtered standard solution and the four diluted solutions (80 uL) were striated on Petri dishes containing LB-agar supplemented with kanamycin (50 μg ml^{-1}) and kept at 37 °C. At the end, the colonies that grew on the solid medium were counted (using the ImageJ software) to estimate the rejection rate of the PAA membranes. The experiments were

performed in duplicate and, as a control, we used the unfiltered standard and four diluted solutions.

3. RESULTS AND DISCUSSION

3.1. Aspects and Optimization of Morphology Parameters of Membranes

Figure 2 shows a PAA membrane after undergoing all the steps described in Figure 1. To guarantee the mechanical stability, as well as to inhibit solution leakage during the filtration, metallic aluminum is maintained at the edge of PPA samples (Fig. 2 (arrow A)). At the center of the image, the partially transparent region corresponds to the PAA membrane itself (Fig. 2 (arrow B)) and the dark ring is the supported membrane on the Al base (Fig. 2 (arrow C)). As described in the experimental section (steps A and E in Fig. 1), the purpose of having different diameters on both side of the aluminum foil is to enhance the mechanical resistance of the filtration ensemble (Fig. 1).

The effects of the different synthesis variables on PAA morphological properties, as well as the rejection rate, were investigated using a 2^3 factorial design. The experimental matrix that we used is presented at Table I, and the experimental conditions are described at same Table. Three different responses were analyzed: D_p, H, and ϕ.

Figure 3 show FE-SEM micrographs from eight experiments described in Table 1 where morphologies obtained with its self-ordered structure could be observed for all PAA membranes.[15] As can be observed in Figure 3, it was possible to control the D_p values, and some of the mean values measured were: 54 ± 11 nm (Fig. 3(c)), 121 ± 11 nm (Fig. 3(h)), and 192 ± 11 nm (Fig. 3(d)), which are in agreement with previous reports. It is important to note that the low quality of the pore ordering is not important for the purposes of this work that is to obtain an inorganic membrane with a mean pore suitable to UF process of *E. coli* bacteria from water. On the other hand, the uniformity of the pores seems remarkable and emphasizes that the procedure described in the experimental section

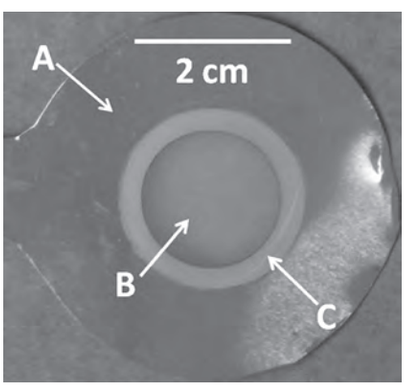

Figure 2. Aluminum foil (arrow A), PAA membrane after all of the steps described in Figure 1 (arrow B), and PAA supported on aluminum (arrow C).

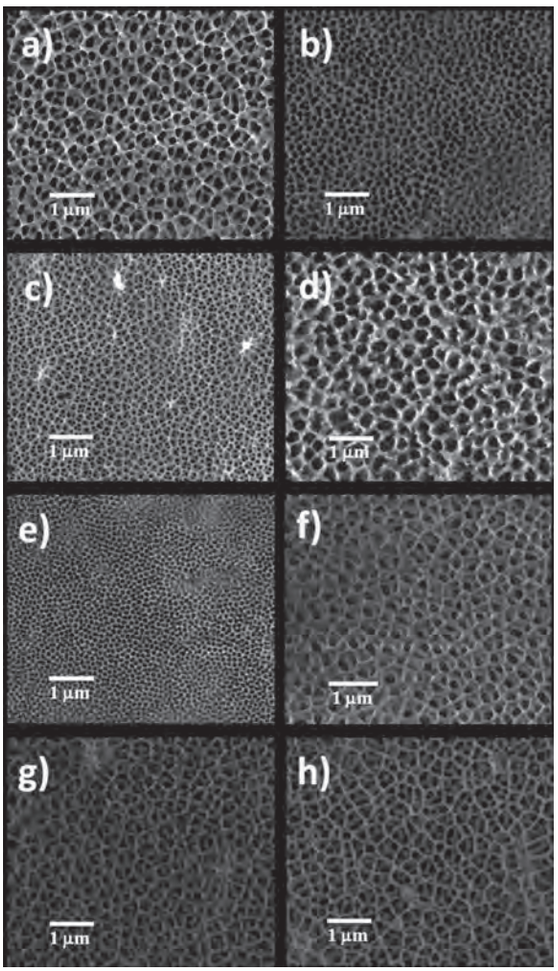

Figure 3. FE-SEM micrographs of PAA membranes showing the pore diameter tuning anodized under distinct conditions described by the 2^3 factorial design. Experiments: #1 (a), #2 (b), #3 (c), #4 (d), #5 (e), #6 (f), #7 (g), and #8 (h), which are described in Table I.

together with the apparatus used for anodizations experiments were essential to keep this uniformity even using a low cost aluminum.

This type of analysis was necessary once the aluminum employed in this work was scarcely investigated in the literature. Kobayashi et al.[10] reported the anodization of aluminum (99.5% purity) in 4 wt% aqueous $H_2C_2O_4$ electrolyte. The authors showed that the porous surface was rather rough in this type of Al tube, but experiments intended to set a tunable size for PAA membranes were not shown by the author. Here we achieve a tunable pore size through combination of three variables in two values, as described in Table I. Other variable could be explored in future work as temperature, other types of electrolytes, other values of current densities or acid concentration to obtain PAA membranes for different purposes. For example, the effect of current density might be much larger for a different electrolyte[36] which highlights the demand for research other experimental conditions to obtain PAA

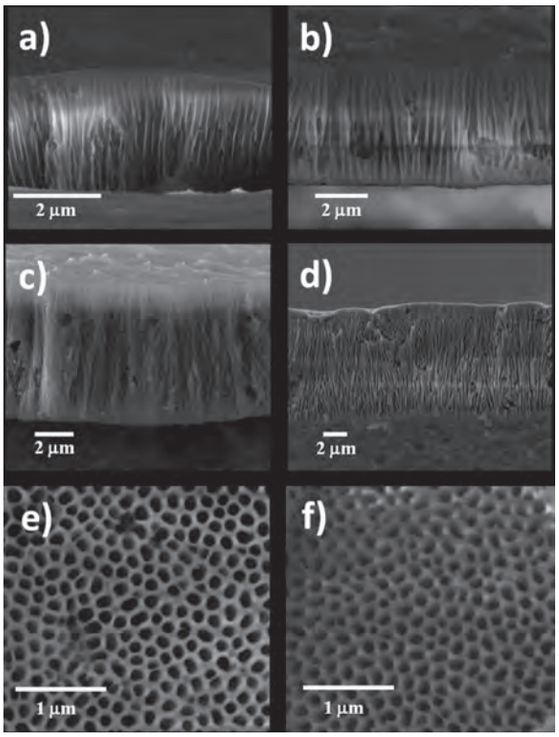

Figure 4. FE-SEM micrographs of PAA membranes showing the membrane thickness tuning during the anodization under distinct conditions described by the 2^3 factorial design of experiment 7 (a), experiment 1 (b), experiment 5 (c), and experiment 8 (d). FE-SEM micrographs of the bottom view of PAA after the removal of the barrier oxide from experiment 2 (e) and experiment 8 (f). All experiments are listed in Table I.

membranes for different purposes using low cost aluminum.

Figure 4 show some of the FE-SEM images from the cross-section that were used to measure the thickness of the PAA membranes. In this Figure, the mean thickness H values were: 2.8 ± 1.0 μm (Fig. 4(a)), 7.7 ± 1.0 μm (Fig. 4(b)), 7.9 ± 1.0 μm (Fig. 4(c)), and 9.3 ± 1.0 μm (Fig. 4(d)). While the pore channels are relatively straight in Figures 4(a)–(c), in some conditions, Figure 4(d), they may be bifurcated. Kopp et al.[45] showed the nanoporous alumina grown on planar, concave, and convex surfaces during the anodization of Al (99.999% purity). In this report, the pore bifurcation occurred when the D_p reached a high value. Moreover, the irregularities in the widened pore bottom refocus the field streamlines, initiating a field-enhanced dissolution of the barrier layer and concluding with the development of branched pores.[45] In our case, how we used low cost Al foils (99.5% purity) in the anodization steps, the pore bottom irregularities could have been caused by impurities in the substrate. Thus, during pore growth we could have the development of branched pores as can be observed in the micrographs of Figures 4(c) and (d).

Another fact that can cause pore bifurcation is the warming of the barrier layer.[15] In trying to reduce this behavior, all measurements were performed with a temperature control under the Al foil to remove the heat generation in the samples,[46] and with mechanical stirring. Without stirring, the electrolyte temperature at the pore bottoms increases significantly and accelerate either chemical dissolution or oxide formation.[36, 40]

Figures 4(e) and (f) show the result of the opening procedure of the barrier layer for experiment 2 and 8, respectively (see Table I). The barrier layer opening was studied and the procedure described in experimental section was enough to remove the barrier layer from the bottom of the pore, thus connecting each side of membrane. These results were similar for the other experimental conditions shown in Table I.

The D_p and H mean values measured for all samples using the 2^3 factorial design are represented in a cube as shown in Figures 5(a) and (b), respectively. This kind of data representation, geometrical representation, it is important to make clear the data showing the changes observed in these responses. The cube axes designate each of the three variables investigated (Table I) and the corners show the results obtained and their respectively SE.

The investigation of D_p is essential since this is the main parameter responsible for affecting the flow rate, as well as the rejection of the bacteria. Therefore, PAA membranes with pore diameters larger than 200 μm are not adequate to achieve this objective. The data presented in Figure 5(a) shows a decrease in the pore diameters as phosphoric acid is exchanged to oxalic acid. It is described in the literature that the uniformity of pore diameter in PAA is heavily affected by the dissolution capability of the acid used in the anodization. Sulka[36] proposed that phosphoric acid is more aggressive to the oxide than oxalic acid, resulting in a significant widening of the pores, as described above. An increment in the current density also results in an increase in D_p values (experiments 2, 4, 6, and 8) because under galvanostatic control at higher currents the potential must be higher and the resulting pore size will be larger.[36] Shawaqfeh and Ahmad[47] showed that n decreases with the anodizing current density by the following relationship:

$$n = n_0 i^{-\alpha} \tag{3}$$

where n is the pore density, i is the current, and n_0 and α are constants.[47] This result is in agreement with the data shown in Figure 5(a).

The effect of the increase in the electrolyte concentration, considering the experimental error, has almost no effect on the D_p values. A factorial design is the only method which allowed us to measure the cross-effects among the variables, such as the effect in the response level of one variable considering the change in a second variable. In this study, we observed a cross-effect between acid concentration and electrolyte type over the response of D_p mean values. In Figure 5(a), it is possible to observe that the D_p values reduced when the acid concentration

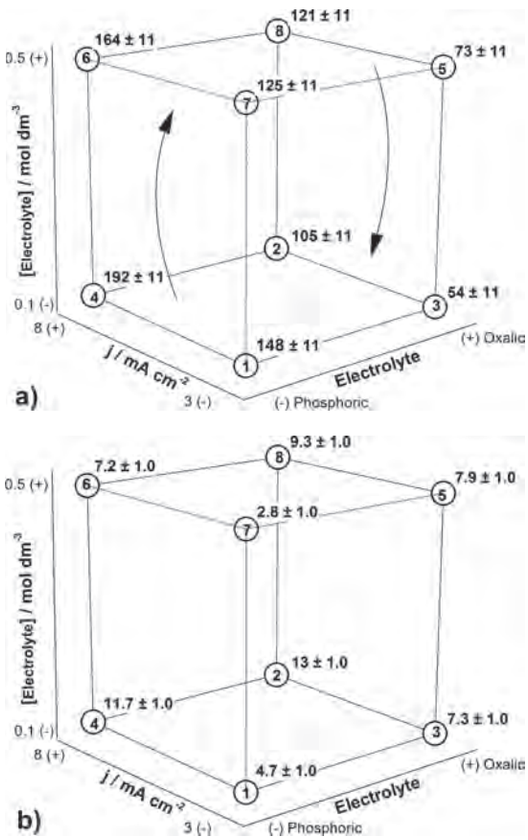

Figure 5. Geometric representation of responses pore diameter (D_p) mean values (nm, a), and film thickness (H) mean values (μm, b) obtained from PAA membranes anodized under the conditions described in Table I. The axes represent the variables investigated: current density, acid concentration, and electrolyte (acid type).

was increased from 0.1 to 0.5 mol L^{-1} in phosphoric acid solution. However, in a different form, their values increase when the concentration of oxalic acid in the solution increased, see arrows in Figure 5(a). A possible explanation could be related to fact that the oxide growth occurs at the oxide/metal interface and, as consequence, anions migrate into the barrier layer due to the electric field.[36] Therefore, different anions can cause this cross-effect.

The H values are showed in Figure 5(b). We observed in this Figure that the greatest thicknesses of the PAA membranes were: 13 ± 1.0 μm (experiment 2), 11.7 ± 1.0 μm (experiment 4), and 9.3 ± 1.0 μm (experiment 8). This parameter could be important for providing a mechanical resistance high enough to make PAA membranes stable during the ultrafiltration process where high pressure can be used.[10, 35] On the other hand, a thicker membrane could increases the mass transfer resistance and would yield lower fluxes. During the experiments, was observed that thick membranes broke with a lower frequency.

The effect of the different variables studied was a decrease in the H vales as electrolyte concentration was increased, which probably related to an increase in the dissolution of the oxide film.[36] The aggressiveness of the phosphoric acid is clearly observed in Figure 5(b), with the H values being considerably smaller (up to 2.8 times lower) when the membranes are prepared in this solution. Finally, when the current density was increased, an increase in the H values was observed.

The results presented in Figure 5 can be used to calculate the effects and interactions of these variables for specific responses (see explanation in the experimental section). Table II shows these results for D_p and H with their respectively SE.

Considering the changes in the D_p, we observed that the main effects were due to the following variables: current density and electrolyte type, with 45.5 ± 11 and -68.5 ± 11, respectively. The negative signal in the latter value indicates that changing the kind of electrolyte from its low level to the high level leads to a "decrease" in the D_p vales. This effect is likely related to the chemical dissolution of the oxide by the electrolyte, as is suggested in the literature.[36] It is important to note that, considering the limit of significance of 25,4, the interactions have any significance effect over D_p values.

Taking into account the film H, all of the main effects were significant. Among them, the most important was the current density effect (4.6 ± 1.0). The positive effects means that we have an increment in the H values when the current density is increased from a low level value to a high level value. This is an expected result since, according to Diggle et al.,[16] the electric field becomes a function of the oxide thickness in order to maintain a constant ionic current density.

Besides to obtain adequate D_p and H values for PAA membranes, to build a filtration system, the water flux is also an important response that will guarantee a large enough quantity of filtrated water. This response will investigate from now on.

3.2. Optimization of Liquid Flux Through of Membranes

Darcy's law and Forchheimer equation,[42] proposed a method to correlate the gas flux (ϕ) with a liquid one. In this sense, gas permeability measurements with N_2 were performed to estimate the output for a liquid ϕ using in the 2^3 factorial design. This procedure was used because of large number of experimental conditions investigated and due to low thickness of some membranes (see Fig. 5(b)), experiment 7 for example) which could crack during flow measurements in liquid. A geometric representation of liquid flux mean values and their main effects and interactions are presented Figure 6(a) and Figure 6(b), respectively. These effects and interactions were analyzed within their limit of significance (i.e. 0.30; Figure 6(b), indicated by dotted lines).

The interaction effect between the current density and electrolyte (acid type) is critical in Figure 6(b), showing a

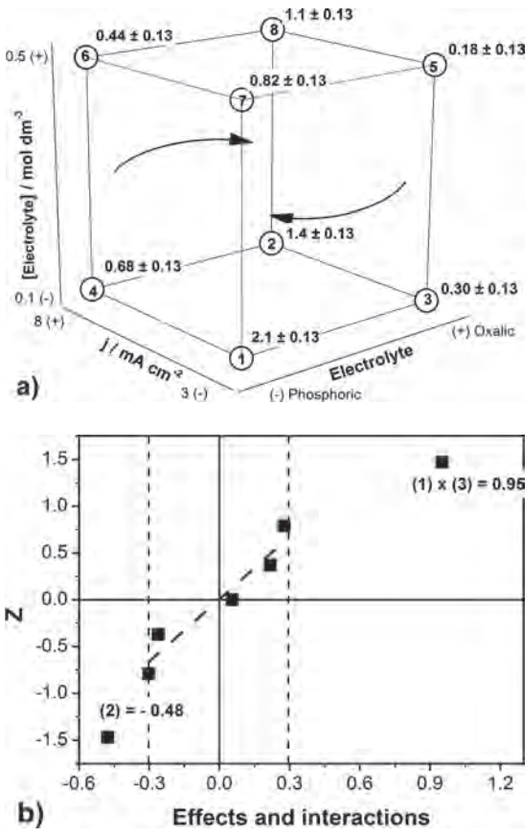

Figure 6. Geometric representation of flux (ϕ) mean values (L h^{-1}; (a) Normal plot of the effects and interactions over flux mean values (L h^{-1}; (b) of PAA membranes anodized under the conditions described by the 2^3 factorial design shown in Table I. Limit of significance (95%): 0.30 (b).

positive effect with 0.95 ± 0.13 significance, followed by a negative effect due to the acid concentration (-0.48 ± 0.13 L h^{-1}). A cross-effect between these two factors is shown in Figure 6(a). This means that at a low current density (3 mA cm^{-2}), when was performed the change from the lower level (phosphoric acid) to the upper level (oxalic acid), we observed a reduction in the liquid flux mean values. However, at high a current density (8 mA cm^{-2}), we have an increment in this parameter with the same level changes, see arrows in Figure 6(a).

The electrolyte and current density were appointed as the main effects to set the best value for the D_p and H (Table II). While for liquid flux, the interaction between them is the principal effect. Finally, the negative value obtained for the acid concentration indicates a decrease in the liquid ϕ when the concentration was changed from 0.1 to 0.5 mol dm^{-3} (Fig. 6(b)). These effects and interactions were analyzed within their limits of significance.

Analyzing all results, D_p, H and liquid ϕ, the PAA membrane prepared in experiments 2 and 8 were the most indicated membranes to next step, the ultrafiltration of *E. coli* bacteria from water.

To test the membranes performance for rejection of pathogens, we conducted a series of experiments using *E. coli*, a typical pathogen in contaminated water, to measure the rejection efficiency. These results will show in the next section for experiment 8. Similar results were obtained for experiment 2 but these data will not be presented here.

3.3. Ultrafiltration of *E. coli* Bacteria from Water with PAA Membranes

The ability of the PAA membrane to remove bacterial contamination from drinking water was tested. The bacteria used in this work was the *E. coli* BL21 strain (typical size 0.5×2 μm), which carries the pET28a plasmid. All experiments were performed in the presence of antibiotic kanamycin. Since *E. coli* BL21 strain could grow on the plates, we were better able to prevent possible contamination that could have hindered the analysis.[44] The Petri dishes with the filtered bacterial concentrate standard with the four dilutions in saline solution (experiments F0 to F4: 10^0, 10^{-1}, 10^{-2}, 10^{-3}, 10^{-4} CFU dm^{-3}) and the unfiltered bacterial concentrate standard with its four dilutions (control, experiments C0 to C4) are shown in Figure 7. Figure 7(a) shows the colonies grown in Petri dishes for the controls when the unfiltered standards were used. Even at low concentrations, we could observe the presence of bacteria colonies. Figures 7(b) and (c) show the Petri dishes prepared with the filtered standard (duplicates of two experiments) at different concentrations. We observed no formation of bacterial colonies in any of the solutions tested. Therefore, the rejection rate of PAA membranes was 100% for the concentrated standard and for the four dilutions. The biological test was successful, and the PAA membrane proved to be completely effective for the removal of dam bacteria *E. coli*.

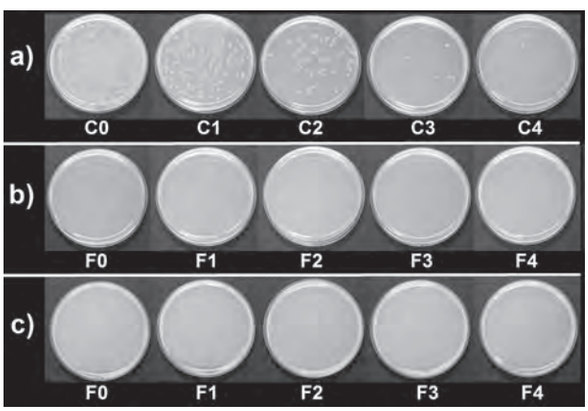

Figure 7. Removal of bacteria using the PAA membrane. Petri dishes with (a) controls, when the unfiltered standard of *E. coli* bacteria solutions were used. C_0 to C_4 corresponds to solutions with 10^0, 10^{-1}, 10^{-2}, 10^{-3}, 10^{-4} CFU dm^{-3}, respectively. Parts (b) and (c) are duplicate experiments using the filtered standard of *E. coli* solutions at different concentrations: F_0 to F_4 corresponding to 10^0, 10^{-1}, 10^{-2}, 10^{-3}, 10^{-4} CFU dm^{-3}, respectively.

4. CONCLUSIONS

It was possible to produce PAA membranes using a low cost aluminum (99.5% purity) with a tunable pore size that was optimized for the rejection of pathogens, such as *E. coli*. The analysis of the responses using the 2^3 factorial design showed that the electrolyte used is the main effect for an optimal D_P to the desired application together with the current density. To increase the H of membrane, the main effect was the current density. Based on flux measurements in N_2, the determining factor for obtaining a high ϕ was the interaction 1–3, between the current density and the electrolyte type, besides the acid concentration used during the anodization step. Finally, using the PAA membrane we produced, it was possible to carry out the physical entrapment of pathogens, such as *E. coli*, thus improving the water quality using a low cost Al.

Acknowledgments: The authors would like to thank FAPESP (process 11/19430-0 and 13/07296-2), CNPq, and CAPES for their financial support.

References and Notes

1. WWAP (World Water Assessment Programme), Green Accounting And Data Improvement For Water Resources: Critical Tools For Informed Decision Making And Sustainable Growth' At World Water (FORUM 6), Marseille **(2012)**.
2. M. M. Khin, A. S. Nair, V. J. Babu, R. Murugan, and S. Ramakrishan, *Energy Environ. Sci.* 5, 8075 **(2012)**.
3. E. E. Geldreich, *Int. J. Food Microbiol.* 9, 295 **(1989)**.
4. N. Das, S. Bandyopadhyay, D. Chattopadhyay, and H. S. Maiti, *J. Mater. Sci.* 31, 5221 **(1996)**.
5. S. V. Jadhav and K. V. Marathe, *Can. J. Chem. Eng.* 91, 311 **(2013)**.
6. W. Pang, N. Gao, and S. Xia, *Desalination* 250, 553 **(2010)**.
7. K. P. Lee and D. Mattia, *J. Membrane Sci.* 435, 52 **(2013)**.
8. N. Maximous, G. Nakhla, W. Wan, and K. Wong, *J. Membrane Sci.* 341, 67 **(2009)**.
9. H. Masuda and K. Fukuda, *Science* 268, 1466 **(1995)**.
10. Y. Kobayashi, K. Iwasaki, T. Kyotani, and A. Tomita, *J. Mater. Sci.* 31, 6185 **(1996)**.
11. D. I. Petukhov, K. S. Napolskii, and A. A. Eliseev, *Nanotechnology* 23, 1 **(2012)**.
12. J. Kim and B. van Der Bruggen, *Environ. Pollut.* 158, 2335 **(2010)**.
13. A. Srivastava, O. N. Srivastava, S. Talapatra, R. Vajtai, and P. M. Ajayan, *Nat. Mater.* 3, 610 **(2004)**.
14. H. Masuda, K. Yada, and A. Osaka, *Jpn. J. Appl. Phys.* 37, 1340 **(1998)**.
15. M. Almasi Kashi, A. Ramazani, M. Raoufi, and A. Karimzadeh, *Thin Solid Films* 518, 6767 **(2010)**.
16. J. W. Diggle, T. C. Downie, and C. W. Goulding, *Chem. Rev.* 69, 365 **(1969)**.
17. T. P. Hoar and N. F. Mott, *J. Phys. Chem. Solids* 9, 97 **(1959)**.
18. J. P. O'Sullivan and G. C. Wood, *Proc. Roy. Soc. Lond. A* 317, 511 **(1970)**.
19. F. Trivinho-Strixino, H. A. Guerreiro, C. S. Gomes, E. C. Pereira, and F. E. G. Guimarães, *Appl. Phys. Lett.* 97, 1 **(2010)**.
20. M. Lillo and D. Losic, *J. Membrane Sci.* 327, 11 **(2009)**.
21. S. Shingubara, *J. Nanopart. Res.* 5, 17 **(2003)**.
22. A. R. Keshavarz, M. Rezaei, and F. Yaripour, *Powder Technol.* 199, 176 **(2010)**.
23. T. Xiu, J. Wang, and Q. Liu, *Micropor. Mesopor. Mat.* 143, 362 **(2011)**.
24. W. Shi, Y. Shen, D. Ge, M. Xue, H. Cao, S. Huang, J. Wang, G. Zhang, and F. Zhang, *J. Membrane Sci.* 325, 801 **(2008)**.
25. P. Kohli, M. Wirtz, and C. R. Martin, *Electroanal.* 16, 9 **(2004)**.
26. A. E. K. Peh and S. F. Y. Li, *Biosens. Bioelectron.* 42, 391 **(2013)**.
27. K. Y. Chan, W. W. Ye, Y. Zhang, L. D. Xiao, P. H. M. Leung, Y. Li, and M. Yang, *Biosens. Bioelectron.* 41, 532 **(2013)**.
28. L. A. Fredin, Z. Li, M. A. Ratner, M. T. Lanagan, and T. J. Marks, *Adv. Mater.* 24, 5946 **(2012)**.
29. L. Li, B. Zhu, S. Ding, H. Lu, Q. Sun, A. Jiang, D. W. Zhang, and C. Zhu, *Nanoscale Res. Lett.* 7, 544 **(2012)**.
30. X. Lu, J. R. G. Evans, and S. N. Heavens, *J. Eur. Ceram. Soc.* 32, 4219 **(2012)**.
31. G. Jeon, S. Y. Yang, J. Byun, and J. K. Kim, *Nano Lett.* 11, 1284 **(2011)**.
32. X. Gao, M. R. Bonilla, J. C. D. da Costa, and S. K. Bhatia, *J. Membrane Sci.* 428, 357 **(2013)**.
33. H. de L. Lira and R. Paterson, *J. Membrane Sci.* 206, 375 **(2002)**.
34. T. Kyotani, W. Xu, Y. Yokoyama, J. Inahara, H. Touhara, and A. Tomita, *J. Membrane Sci.* 196, 231 **(2002)**.
35. K. Itaya, S. Sugawara, A. Kunio, and S. Saito, *J. Chem. Eng. Japan* 9, 514 **(1984)**.
36. G. D. Sulka, Nanostructured Materials In Electrochemistry, Wiley-VCH, Weinheim **(2008)**.
37. G. Patermarakis and K. Moussoutzanis, *J. Electroanal. Chem.* 659, 176 **(2011)**.
38. W. Lee, R. Ji, U. Gösele, and K. Nielsch, *Nat. Mater.* 5, 741 **(2006)**.
39. E. R. Bruns, I. S. Scarminio, and B. B. Neto, Statiscal Design-Chemometrics, Elsevier Science, Amsterdan **(2006)**.
40. F. Li, L. Zhang, and R. M. Metzger, *Chem. Mater.* 10, 2470 **(1998)**.
41. C. P. Oliveira, M. L. Cardoso, A. J. A. Oliveira, and E. C. Pereira, *J. Nanosci. Nanotechnol.* 9, 6487 **(2009)**.
42. Z. Wen, G. Huang, and H. Zhan, *Hydrogeol. J.* 19, 1 **(2011)**.
43. G. E. P. Box, J. S. Hunter, and W. G. Hunter, Statistics for Experiments: Design, Innovation, And Discovery, 2nd Edition, John Wiley and Sons, New Jersey **(2005)**.
44. J. Sambrook, E. Fritsch, and T. Maniatis, Molecular Cloning: A Laboratory Manual, Cold Spring Harbor Laboratory, New York **(1989)**.
45. O. Kopp, M. Lelonek, and M. Knoll, *J. Phys. Chem. C* 115, 7993 **(2011)**.
46. G. Patermarakis and N. Papandreadis, *Electrochim. Acta* 38, 2351 **(1993)**.
47. A. T. Shawaqfeh and R. E. Baltus, *J. Membrane Sci.* 157, 147 **(1999)**.

Received: 15 December 2014. Accepted: 6 March 2015.